

EXPERIMENTAL CHARACTERIZATION OF THE COHERENT HARMONIC GENERATION SOURCE AT THE DELTA STORAGE RING *

M. Huck[†], M. Höner, H. Huck, S. Khan, R. Molo, A. Schick, P. Ungelenk,
Center for Synchrotron Radiation (DELTA), TU Dortmund University, Dortmund, Germany
S. Cramm, L. Plucinski, C.M. Schneider, Forschungszentrum Jülich (FZJ) PGI6, Jülich, Germany
S. Döring, Fakultät Physik, Universität Duisburg-Essen, Duisburg, Germany

Abstract

The short-pulse facility at the 1.5-GeV synchrotron light source DELTA, operated by the TU Dortmund University, generates coherent VUV and THz radiation by Coherent Harmonic Generation (CHG). Here, a femtosecond laser pulse interacts with an electron bunch in an undulator causing a periodic energy modulation and subsequent microbunching, which gives rise to coherent radiation at harmonics of the seed wavelength. Rather than using Ti:Sapphire laser pulses at 795 nm directly, the second harmonic is employed for seeding since 2012. After significant modifications of the seed laser beamline and the dispersive chicane to improve the microbunching, the last commissioning steps include characterization of the CHG radiation and preparing the experimental setup at an existing VUV beamline for time-resolved photoemission spectroscopy. In this paper, the status of the project and recent experimental results are presented.

INTRODUCTION

DELTA is a 1.5-GeV synchrotron radiation source operated by the Center for Synchrotron Radiation at the TU Dortmund University. The source for ultrashort VUV pulses based on the CHG principle [1] is in operation at DELTA since 2011 [2–5]. The layout is shown in Fig. 1.

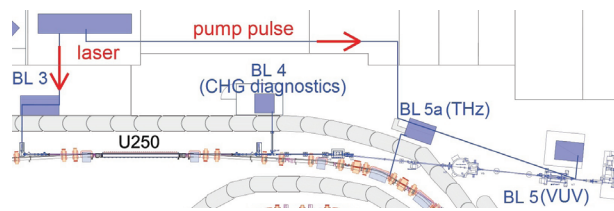


Figure 1: The layout of the CHG facility at DELTA.

A Ti:Sapphire femtosecond laser system is used for seeding, initially with its standard wavelength of 795 nm. Since 2012, the second harmonic generated with a nonlinear crystal is employed. The laser is focused by a telescope at beamline 3 (BL 3) into the undulator (U250). Initially, the telescope was built of three lenses, but for seeding with 398 nm they were replaced by curved mirrors to minimize the effect of group-delay dispersion that expands the temporal profile of the pulses at short wavelengths. The undulator consists of three parts with separate power supplies,

* Work supported by DFG, BMBF, and by the Federal State NRW.

[†] Maryam.Zeinalzadeh@tu-dortmund.de

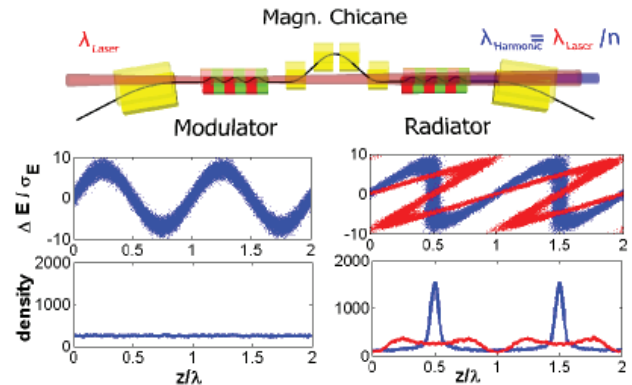


Figure 2: Optical klystron configuration and CHG principle. Energy and density modulation in the modulator (left) and after passing the chicane (right, for two different chicane strengths) are shown in longitudinal phase space.

namely modulator, dispersive chicane and radiator. This configuration is called Optical Klystron (Fig. 2). In the modulator, the electric field of the laser pulse modifies the energy of the electrons periodically in a small slice of the bunch (10^{-3} of its length). The dispersive chicane causes the modulated electrons to travel on trajectories of different length and hence to form microbunches, which radiate coherently in the radiator. The main parameters are shown in Table 1.

The radiation wavelength can be chosen by tuning the radiator to harmonics of the seed wavelength. Finally, the CHG radiation is sent either via BL 4 to a diagnostics hutch for optimization and characterization, or to a VUV beamline (BL 5) for detection and application in user experiments. A few meters downstream of the undulator, path length dif-

Table 1: Specifications of CHG facility at DELTA

bunch length (FWHM)	~ 100 ps
single-bunch current/charge	up to 20 mA / 8 nC
revolution frequency	2.6 MHz
undulator period	250 mm
number of periods	17
K value of modulator/radiator	0 - 11
r_{56} of the chicane	0 - 130 μm
laser pulse energy @398 nm	up to 2.8 mJ
pulse duration (FWHM)	$\sim 40 - 70$ fs
laser repetition rate	1 kHz

ferences of the off-energy electrons cause a sub-millimeter gap in the density profile of the electron bunch which leads to the emission of the coherent THz radiation. The coherent THz radiation is extracted via a dedicated beamline (BL 5a) and can be used as a diagnostics tool for CHG experiments, as well as for time-resolved far-infrared spectroscopy [6]. A dedicated beamline has been constructed to guide a fraction of the laser pulses to the experimental stations at BL 5 and BL 5a for the purpose of pump-probe experiments.

IMPROVEMENTS AND RESULTS

The degree of microbunching depends on the strength of the chicane r_{56} and on the laser pulse energy E_L . In order to obtain the optimum microbunching, the relation $\lambda_L/4 \approx r_{56}\Delta E/E$ must hold, in which λ_L is the seed wavelength and $\Delta E/E$ the energy modulation amplitude of the electrons. Since the energy modulation is limited by the available laser pulse energy and ultimately by the energy acceptance of the storage ring, the chicane strength is the key parameter to achieve the optimum microbunching.

Modification of the Magnetic Chicane

Until the beginning of 2013, the r_{56} value was limited to 11 μm . It was increased up to 130 μm by modifying the chicane, which caused a dramatic rise in the intensity of the CHG radiation. The magnetic chicane was initially formed by three undulator periods with an increased magnetic field. By rewiring the poles of the chicane, thus changing the longitudinal profile of the magnetic field, a much larger transverse excursion is created which leads to higher values of r_{56} . Further details are explained in [7]. The relationship between the CHG intensity and chicane strength can be written as [8]

$$I_{\text{CHG}} \propto f_n^2 J_n^2 (4\pi n(N_u + N_d)(\Delta E/E))$$

$$\text{with } f_n = e^{-8(\pi n(N_u + N_d))\sigma_\gamma^2}, \quad (1)$$

where n is the harmonic number, σ_γ is the relative energy spread of the electrons (roughly equal to $7 \cdot 10^{-4}$), N_u is the number of undulator periods, $N_d = r_{56}/(2\lambda_L)$ is the number of undulator-equivalent periods of the dispersive chicane, J_n is the n -th-order Bessel function, and f_n is the modulation depth.

The measured CHG signal versus chicane strength is shown in Fig. 3 for two laser pulse energies. The green points in Fig. 3a represent the data obtained with the old chicane showing the limitations of that configuration. There is a good match between the measured data and the fit to Eq. (1). As the chicane strength increases, the CHG intensity also increases and reaches a maximum around $r_{56} = 23 \mu\text{m}$ and $43 \mu\text{m}$, respectively, for $E_L = 2.6 \text{ mJ}$ and 1.3 mJ . Further increasing the chicane strength causes another peak appearing beyond the first maximum, which corresponds to overbunching and the formation of the double-peak structure in the longitudinal density distribution (Fig. 2). By fitting the measured CHG signal versus

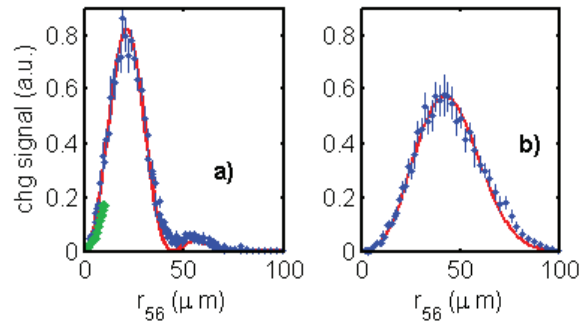


Figure 3: CHG intensity vs. chicane strength a) for a laser pulse energy of $E_L = 2.6 \text{ mJ}$ and b) for $E_L = 1.3 \text{ mJ}$.

r_{56} with Eq. (1), an "effective" energy modulation as function of the laser pulse energy can be deduced. As shown in Fig. 4, the energy modulation is proportional to the square root of the laser pulse energy, which is consistent with the theory [8]. The discrepancy between simulation and measured data can be attributed to non-perfect laser settings and beamline transmission.

Photoelectrons from CHG Pulses

As an important step towards user application, CHG radiation was detected in BL 5 which is presently the only way to study CHG pulses below 200 nm, since an evacuated beamline is required.

BL 5 is operated by the Forschungszentrum Jülich. It is equipped with a plane grating monochromator (PGM), a photoelectron spectrometer and a delay-line detector (DLD) [11, 12], and is operated in the VUV and soft x-ray regime for angular- and spin-resolved photoelectron spectroscopy. In order to detect the CHG pulses, the timing capability of the DLD was enabled. The time resolution is not limited by the DLD, but by the temporal broadening due to different photoelectron trajectories inside the spectrometer, which result in an accumulated pulse width of about 50 ns (FWHM). This is sufficient to resolve CHG signals in successive single-bunch turns (Fig. 5) and also to perform CHG experiments with a hybrid fill pattern. The ratio between photoelectron counts from a gold target due to CHG and due to spontaneous radiation was about 600 and 150 at 199 nm and 133 nm, respectively. Since the U250 is tuned to deflection parameters of $2.8 < K < 7.2$, the radiation not only includes the fundamental wavelength, but also strong harmonics, which pass the PGM due to high-

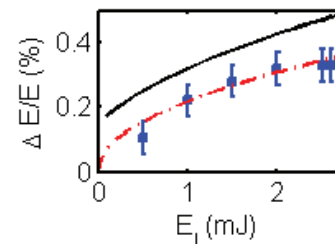


Figure 4: Effective energy modulation amplitude versus laser pulse energy. The solid line is obtained by particle tracking simulation [10].

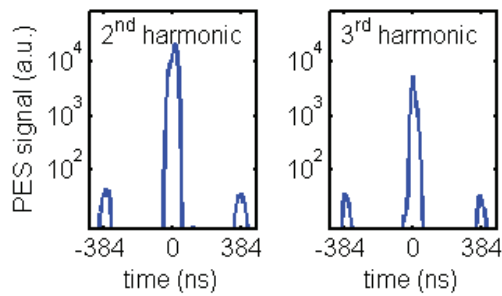


Figure 5: CHG (at $t = 0$) and spontaneous emission (at $t = \pm 384$ ns) signal from photoelectrons detected by the DLD at $\lambda = 199$ nm (left) and $\lambda = 133$ nm (right).

order diffraction. To exclude the higher harmonics, a LiF filter with a cutoff wavelength of about 120 nm is used. In order to detect the fourth and fifth harmonic (100 and 80 nm, respectively) the LiF filter was removed. CHG pulses at both harmonics have been observed, but the strong high-order background requires further studies. The CHG spectra at the second (Fig. 6a) and third (Fig. 6b) harmonic were detected by changing the PGM pass wavelength. The results are consistent with those from other measurements using a Czerny-Turner spectrometer equipped with an avalanche photodiode (APD) [9] (Fig. 6c) and a CCD-array spectrometer (Fig. 6d). Assuming a pulse duration of 50 fs, the time-bandwidth product is only a factor of two larger than the Fourier limit.

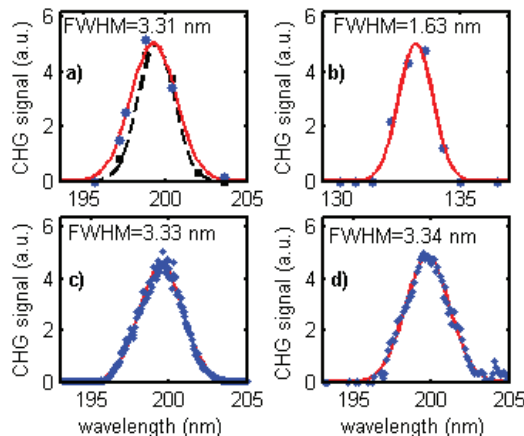


Figure 6: CHG spectra at the second/third harmonic obtained using photoelectrons under variation of the PGM wavelength (a, b), a Czerny-Turner spectrometer equipped with an APD (c), and a linear CCD array spectrometer (d). The dashed curve was measured with a smaller PGM exit slit ($600 \mu\text{m}$), yielding a smaller width (2.62 nm).

Transverse Coherence Measurement

First double-slit experiments to study the transverse coherence were performed. The interference pattern is measured by a fast-gated intensified CCD camera [14]. An example is shown in Fig. 7, in which the slit width is 0.1 mm, the slit separation is 0.5 mm and the distance from the slits to the screen is 1 m. A preliminary analysis yields a central

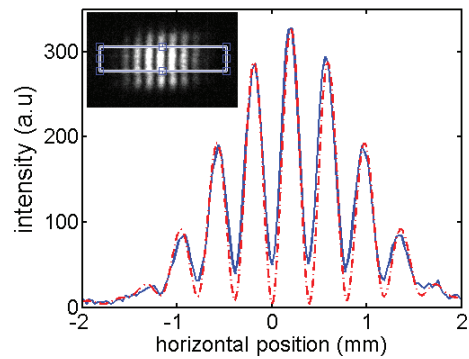


Figure 7: Measured (solid line) and fitted (dashed line) interference pattern of CHG radiation at 199 nm obtained with a double-slit experiment.

visibility of the fringes of 0.76 (\approx coherence degree of the radiation).

SUMMARY AND OUTLOOK

By modifying the chicane and achieving higher r_{56} values, a dramatic increase in the CHG signal was observed. The CHG pulses up to the fifth harmonic were detected using a photoelectron spectrometer. Seeding with 265 nm is the next step to generate lower wavelengths for pump-probe experiments at BL 5. For even lower wavelengths the EEHG [13] scheme is planned to be implemented at DELTA.

ACKNOWLEDGMENT

We are pleased to thank our colleagues at DELTA and in other institutes particularly, FZJ/Jülich, HZB/Berlin, DESY/Hamburg and KIT/Karlsruhe, for their continuous support and advices. The financial supports of DFG, BMBF and NRW Forschungsschule is gratefully acknowledged.

REFERENCES

- [1] R. Coisson and F. D. Martini, Phys. of Quant. Electron. 9, 939 (1982).
B. Girard et al., Phys. Rev. Lett. 53, 2405 (1984).
M. Labat et al., Phys. Rev. Lett. 101, 164803 (2008).
E. Allaria et al., Phys. Rev. Lett. 100, 174801 (2008).
- [2] S. Khan et al., Sync. Rad. News 24, 18 (2011).
- [3] H. Huck et al., Proc. FEL 2011, Shanghai, 5.
- [4] A. Schick et al., Proc. IPAC 2012, New Orleans, 1617.
- [5] H. Huck et al., Proc. FEL 2012, Nara, 12.
- [6] P. Ungelenk et al., this conference (MOPEA014).
- [7] R. Molo et al., this conference (TUPWO007).
- [8] M. Labat et al., Eur. Phys. J. D 44, 187 (2007).
- [9] The APD was set up by K. Holldack, HZB Berlin.
- [10] M. Höner et al., Proc. IPAC 2011, San Sebastian, 2939.
- [11] L. Plucinski et al., J. Electron Spectros. Rel. Phenom. 181, 215 (2010).
- [12] www.surface-concept.com
- [13] G. Stupakov, Phys. Rev. Lett. 102, 074801 (2009).
- [14] The camera was provided by B. Schmidt and S. Wunderlich, DESY, Hamburg.